Mini Review

Progress in the Structural Design of a Titanium Dioxide Membrane and its Photocatalytic Degradation Properties

Xu Xue-li, Song Wei[*]

School of Biological and Chemical Engineering, Nanyang Institute of Technology, NO.80 Changjiang Road, Nanyang, Henan, China, 473004
[*]E-mail: song78wei@163.com

A great deal of attention has recently been paid to degrading polluted water using titanium dioxide because it has the characteristics of low price, nontoxicity and extensive wastewater. However, its wide energy gap, high composite rate of photoelectrons and holes, and difficult separation from wastewater limit its wide application. To improve the photocatalytic property of titanium dioxide and simplify the wastewater treatment process, recent progress in the effect of ion/atomic doping on the photocatalytic activity of titanium dioxide and the applications of solidification technology in the preparation of titanium dioxide members have been discussed, and urgent issues for future research and development are proposed.

1. INTRODUCTION

With the continuous intensification of anthropogenic industrial activities, environmental problems have become increasingly serious. Since Fujishima and Honda [1] first discovered in 1972 that titanium dioxide (TiO_2) could undergo redox reaction with water under light conditions, TiO_2 has attracted extensive attention from numerous scientists owing to its advantages, such as nontoxicity, no secondary pollution, low price and theoretically unlimited use. These scientists attempted to use it in the advanced treatment of drinking water and dye wastewater [2-4]. The study of TiO_2 degradation of pollutants is shown in Table 1. TiO_2 has been proven to be an efficient photocatalyst for the selective elimination of environmental pollutants. However, it responds primarily to UV light; for technoeconomic reasons, it is important that visible-light-driven photocatalysts with high efficiency be developed.

Table 1. Effect of TiO_2 on the photocatalytic degradation of organic pollutants

Operating condition	Pollutants	Degradation rate	Reference
3 h natural light irradiation	Methyl Blue	>90%	[5]
200 min UV-light irradiation	Methyl Orange	>80%	[6]
2 h UV-light irradiation	Methyl Blue	>99%	[7]
240 min visible light irradiation	Rhodamine B	>60%	[8]
1 h UV light irradiation	Organic Vapors (Benzene, toluene, ethyl benzene, and xylene)	>90%	[9]
40 min UV-light irradiation	Phenol	>66.8%	[10]
20 min visible-light irradiation	Gaseous Acetone	>99%	[11]
3 h UV-light irradiation	Organic Acid	>68.6%	[12]
20 min UV light	Caffeine	>99%	[13]
50 min UV-light irradiation	Acetaldehyde	>85%	[14]
12 h UV-light irradiation	Methyl Orange	>99.9%	[15]
1 h solar light	Gaseous Butane	>90%	[16]
40 min Visible-light irradiation	Escherichia coli K12	>65.9%	[17]
12 h UV-light irradiation	Diphenhydramine	>90%	[18]
5 h Visible-light	Sulfate-Reducing Bacteria	>56.3%	[19]
1 h Visible-light with 1000 W Xenon lamp	Trichlorophenol	87.8%	[20]

In Fig. 1, the light-excited photocatalytic reaction process of TiO_2 is displayed. Given the wide band gap of the TiO_2 photocatalyst (E_g= 3.2 eV, λ= 387 nm), it can only absorb ultraviolet (UV) light with wavelengths less than 387 nm, which account for only 4–6% of the sunlight wavelengths [21]. In early research concerning photocatalytic wastewater treatment with TiO_2, suspension systems were mainly used, which led to problems such as the easy loss of TiO_2 and difficult separation. Moreover, the light absorption and blocking by suspended TiO_2 particles in wastewater also affected the radiation depth of light, thereby restricting the further extensive application of TiO_2 photocatalysts. To broaden the photoresponse range of TiO_2, enhance its photocatalytic efficiency and simplify the treatment process, numerous researchers around the world have carried out a series of studies on the composition regulation of TiO_2 and the preparation of TiO_2 membranes, which are reviewed below.
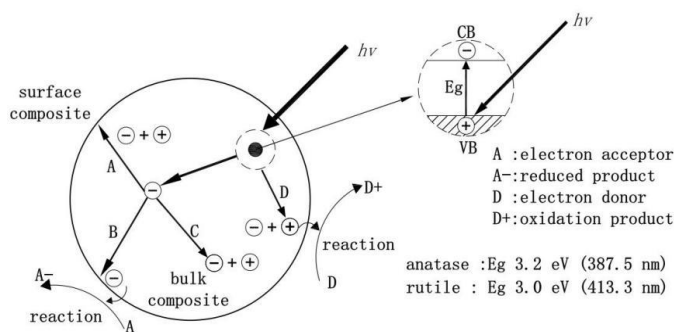

Figure 1. Mechanism of the photocatalytic reaction of TiO_2 excited by light[22]

2. COMPOSITION REGULATION OF TiO₂

2.1. Crystal structure of TiO₂

The TiO₂ used in photocatalysis is often in the rutile and anatase forms, whose crystal structures are displayed in Fig. 2. Although both are composed of titanium–oxygen octahedrons, anatase TiO₂ has a lower density (3.894 g/cm^3 vs. 4.250 g/cm^3) and a wider band gap (3.2 eV vs. 3.0 eV) than rutile TiO₂ since it is connected by common edges and common points [23]. Additionally, anatase TiO₂ has rhombic tunnels in its crystal structure along the [010] and [100] directions, which thus has a macroporous structure on its surface.

Moreover, its crystal structure is asymmetric, thus better facilitating the generation and separation of photogenerated electrons. So it is photocatalytically more active than rutile TiO₂ [24]. Nevertheless, anatase TiO₂ has a slightly worse catalytic stability than rutile TiO₂ due to its metastable structure. To improve the photoresponse range of TiO₂, prolong its life cycle and enhance its catalytic efficiency, measures such as ion doping [25], noble metal deposition [26], semiconductor photosensitization and semiconductor compounding are currently adopted to regulate its composition.
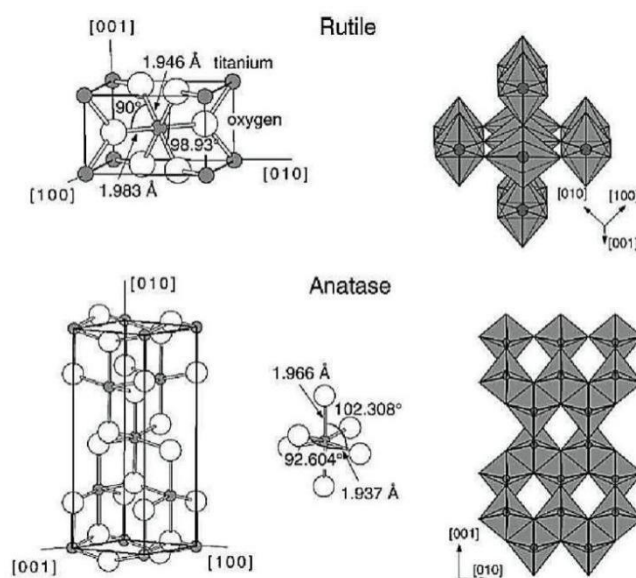

Figure 2. (a) Rutile and (b) anatase structures of titanium dioxide[24]

2.2. Ion doping

By physically or chemically introducing ions into the target semiconductor lattice, the distortions and defects of the TiO₂ lattice can be promoted. Fig. 3 displays the changes in the energy band structure of TiO₂ doped with different ions.
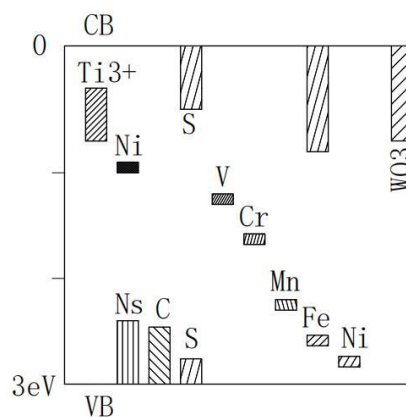
Figure 3. Energy gap of titanium dioxide doped with different ions[27]

It is clear that the alteration of the TiO$_2$ energy band structure by introduced foreign ions is the most deeply investigated and most widely used method for improving the photocatalytic performance of TiO$_2$ [28-30]. Depending on the mode of implementation, ion doping can be classified into during treatment and after treatment. During treatment, ion doping is implemented simultaneously with TiO$_2$ formation, while after treatment, ion doping is implemented after the formation of the TiO$_2$ catalyst. Ion doping can also be classified into single doping and codoping depending on the number of doped ions and into M^{x+} doping and nonmetal ion doping depending on the type of ions. Generally, with metal ion doping, Ti^{4+} ions in the lattice are replaced to form M–O–Ti bonds, while with nonmetal ion doping, N$_y^-$ replaces O^{2-} ions in the lattice to form Ti–N$_y$–Ti bonds or exists in the TiO$_2$ lattice gaps as interstitial molecules/ions. The introduction of doped ions facilitates the generation of TiO$_2$ oxygen vacancies and other defects, thereby promoting carrier separation.

2.2.1. Metal ion doping

Transitional or rare earth element ions are normally used in metal ion doping. Doping of transitional metal ions into the TiO$_2$ lattice promotes an increase in the number of TiO$_2$ defects. Given their multiple valence states, the transition metal ions doped into TiO$_2$ can act as traps for photogenerated carriers. When the traps are shallow, the separation of carriers is facilitated, thereby promoting the improvement of TiO$_2$ catalytic efficiency. When the traps are deep, they become the recombination center of carriers, thereby leading to the degraded photocatalytic performance of TiO$_2$ [31]. When doped metal ions are 3d transition elements represented by Cr, Co, Ni, etc., new energy levels can be generated in the original forbidden band of TiO$_2$, resulting in a redshift of the TiO$_2$ absorption wavelength [32]. Hoffman [33] prepared metal ion-doped TiO$_2$ by the sol–gel process and systematically investigated the effects of various (21 types) transitional metal doping treatments on the catalytic performance of TiO$_2$. Their results showed that the metal ions represented by Fe^{3+} and Ru^{2+} were conducive to improving the TiO$_2$ catalytic performance. The metal ions represented by Cr^{3+} and Ni^{2+} reduced the photocatalytic performance of TiO$_2$, and the transition metal ions represented by Ga^{3+} and Zn^{2+} had little impact on the photocatalytic performance of TiO$_2$. Notably, at excessively high doping concentrations, the transition element ions became the recombination center of carriers, which

aggravated the carrier separation to reduce the catalytic performance of TiO_2 instead.

Rare earth elements feature good photocatalytic performance owing to their incompletely occupied 4f orbitals and empty 5d orbitals, which are thus widely used in the photocatalytic modification and regulation of semiconductor catalysts [34]. Doping of rare earth elements can elevate the phase transition temperature of anatase TiO_2 and enhance the thermal stability of the catalyst. It can also alter the ligand field of TiO_2 and narrow its forbidden bandwidth. In addition, rare earth elements can improve the number of Lewis base centers on the TiO_2 surface as well, which facilitates an increase in the number of TiO_2 adsorption centers. Xu [35] used rare earth precursors as a doping source to prepare rare earth-doped TiO_2 nanoparticles by a sol–gel process, which greatly increased the photoresponse range of TiO_2. Furthermore, they analyzed the redshift after doping TiO_2 with rare earth ions and discovered the following rule: $Gd^{3+} > Nd^{3+} > La^{3+} > Pr^{3+} \approx Er^{3+} > Ce^{3+} > Sm^{3+}$, which was in the opposite order of the rare earth ion radii, suggesting that the ionic radius is the major factor influencing the doping doses of rare earth ions in the TiO_2 lattice. After rare earth doping of TiO_2, the catalytic degradation of nitrite can be achieved within the visible light range.

2.2.2. Nonmetal ion doping

Nonmetal ion doping can significantly reduce the forbidden bandwidth of TiO_2 and increase its range of light wave absorption. Currently usable nonmetals include N, C, P, S, B and F, of which N doping is the most investigated. Although nonmetal ion doping has been widely accepted since it can reduce the forbidden bandwidth of TiO_2 and improve its photocatalytic response range [36], there remains no consensus on the mechanism whereby nonmetal ions broaden the photoresponse range of TiO_2. Rather extensive existing mechanism models include the fixed energy level theory represented by Nakamura [37] (holding that the doped ions form new impurity energy levels that are characterized by isolation and fixedness), the localized energy level theory represented by Di valentin [38] (believing that at high concentrations of nonmetal dopant ions, new localized energy levels can be formed above the O2p level of TiO_2, which can well explain Batzill's [39] experimental results), and the hybrid energy level theory represented by Asahi [40] (through density functional theory, Asahi explored the orbital energy variations after doping of nonmetal elements into the TiO_2 lattice, finding that the reduction of TiO_2's forbidden band width was caused by hybridization of its O2p orbital with the p orbital in the nonmetal and that the position of the hybrid orbital depended on the concentration of doped ions). The higher the doped ion concentration is, the higher the energy level of the hybrid orbital, the smaller the forbidden band width, the larger the absorption cutoff wavelength, and the more significant the redshift of TiO_2. The oxygen vacancy theory is represented by Ihara [41] (holding that the doped ions occupy the oxygen vacancies in the TiO_2 lattice to prevent their reoxidation, thereby leading to the redshift of TiO_2). The impurity sensitization theory is represented by Sato [42] (holding that the doped impurities endow TiO_2 with visible light catalytic properties). Although nonmetal doping can enhance the photocatalytic activity of TiO_2, the treatment process is mostly implemented under vacuum and high temperature conditions, which are thus complicated and expensive. In addition, the catalyst stability can hardly be ensured.

2.2.3. Rare earth ion–nonmetal ion codoping

Since rare earth element ions can promote the separation of photogenerated electrons and improve the photon quantum yield, whereas nonmetal ions can broaden the photoabsorption capacity of TiO_2, codoping of appropriate rare earth elements and nonmetal ions into TiO_2 is conducive to enhancing the photocatalytic performance of TiO_2 through the synergistic effect between the two dopants [43][44]. Through a sol-gel process, Sakatani [45] doped TiO_2 powder simultaneously with La and N and found that codoped TiO_2 achieved photocatalytic degradation of acetaldehyde under visible light. Wu [46] compared the methyl orange-degrading effects between Ce–N codoped and N-doped TiO_2, which revealed a higher photocatalytic efficiency of the codoped TiO_2. Given the limited source of rare earth raw materials and the substantial wastewater treatment, it is difficult to actually apply codoping to industrial production.
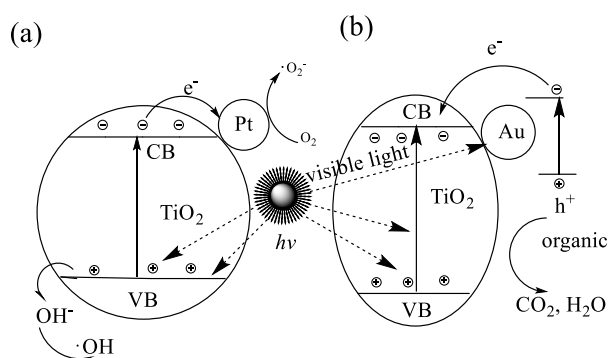
2.3. Noble metal deposition

Figure 4. Mechanism of electron-hole separation on the surface of titanium dioxide: (a) Pt/TiO_2 and (b) Au/TiO_2[53]

Fig. 4 describes the mechanism whereby noble metals promote electron–hole separation on the TiO_2 surface. Since noble metals (Ag [47], Au [48], Ru [49], Pt [50] and Pd [51]) have lower Fermi energy than TiO_2, deposition of noble metal nanoparticles onto the TiO_2 surface can facilitate the migration of electrons in TiO_2 toward the noble metal particles, thereby promoting effective electron–hole separation in TiO_2 to improve TiO_2's photocatalytic activity. Common techniques for noble metal deposition include surface sputtering [52], impregnation reduction [53], electrodeposition [54] and photoassisted induction [55]. Apart from decreasing the specific surface area of catalysts, noble metal deposition can also affect the selectivity of TiO_2 photocatalysts. The deposition amount and particle size distribution of noble metals are important factors influencing catalyst performance. Kong [56] fabricated Ag-loaded TiO_2 nanorods by bipotential codeposition. Their results showed that after Ag loading, charge carrier recombination by the catalyst was evidently inhibited, which could improve the photocatalytic reduction efficiency of TiO_2 by 5 times. Nevertheless, the high price and low surface area of noble metals limit their wide application in wastewater treatment.

2.4. Semiconductor photosensitization

By adsorbing a photosensitizer on the TiO_2 surface, a photosensitized TiO_2 photocatalyst can be prepared. When the excited state potential of the photosensitizer is lower than the conduction band potential of the semiconductor, the photogenerated electrons on the photosensitizer surface are possibly injected into the conduction band of TiO_2, which then migrate onto the catalyst surface, thereby broadening the photoabsorption wavelength range of the TiO_2 catalyst. Photosensitizers can be classified into two types: organic and inorganic. Organic photosensitizers mainly include chlorophyllin [57] and rose bengal [58], which have a good photosensitization effect but a poor binding force with TiO_2. Meanwhile, inorganic photosensitizers are primarily complexes of various noble metals [59], which have limited application due to their complicated preparation process and high price. Regardless of whether the photosensitizer is organic or inorganic, it has a competitive adsorption relationship with TiO_2 and organic matter to be degraded, which thus affects the number of TiO_2 active centers and reduces the active specific on the surface area.

3. PREPARATION OF TiO₂ MEMBRANES

Since powdered TiO_2 was mostly used for the TiO_2 photocatalytic degradation of polluted wastewater in the early days, while the research on the loading method of active catalyst components is rather mature, many researchers have loaded TiO_2 powders on carriers to increase the active center number of TiO_2 and prolong its life cycle. Currently, carriers such as alumina [60], zeolite [61], silica gel [62], stainless steel wire mesh [63], optical fiber [64] and plexiglass [65] are mainly used around the world. Meanwhile, the sources of immobilized TiO_2 are primarily TiO_2 powder [66], TiO_2 precursor [67] or titanium metal [68], and the common techniques for TiO_2 immobilization include the sol–gel process, electrophoretic deposition, hydrothermal synthesis, chemical vapor deposition and anodization.

3.1. Sol-gel process

TiO_2 sol is prepared through reactions (e.g., hydrolysis and condensation) of titanium alkoxides or their inorganic salts (as the raw material) under acidic conditions, and Fig. 5 illustrates the relevant preparation process. During the gelation process by aging, TiO_2 sol is loaded onto the carrier by means of impregnation, dip coating or spraying. In this way, TiO_2 precursor-loaded photocatalysts can be prepared, which is currently the most common method of preparing immobilized TiO_2 photocatalysts in experimental research. Exploiting this technique, Yu [69] et al. prepared TiO_2 photocatalysts on glass, which could effectively degrade dimethyl dichloro-vinyl phosphate under sunlight. However, there are numerous factors affecting the preparation of TiO_2 membranes by this technique, such as the wide particle size distribution and long production cycle of TiO_2, as well as the poor bonding force between TiO_2 and the substrate, which thus remains in the laboratory research stage.
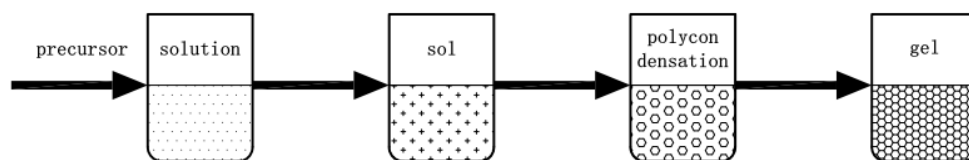
Figure 5. Preparation process of titanium dioxide by the sol-gel method[10]

3.2. Electrophoretic deposition

During the immobilization of TiO_2 with Pt [70], C [71], conductive glass [72] and stainless steel [73] (as the substrate material), the highly dispersed TiO_2 nanopowder can be immobilized on the substrate under electric field force by using the substrate material as the cathode. Since the TiO_2 membrane is prepared under electrochemical action, the quality of the membrane is closely linked to the power supply parameters. Limited by the power supply conditions, it is difficult to prepare a large-area TiO_2 membrane by this technique. In addition, to ensure the continuity of the current, the substrate material needs to be conductive, thus narrowing the material choice. Mostly, electrophoretic deposition is used for the preparation of photovoltaic cell electrodes or electrically assisted photocatalysts.

3.3. Chemical vapor deposition

With this method, titanium-containing alkoxide or inorganic salt is used as the titanium source [74], which is vaporized by heating and deposited on the carrier surface in an inert gas. Under thermal action, the decomposition of titanium salt is promoted to form TiO_2 membranes. The bonding force between the TiO_2 membrane (prepared by chemical vapor deposition) and substrate is low and decreases as the coating thickness increases. Moreover, the preparation of TiO_2 membranes by this technique needs to be implemented at high temperature, the process is complicated, and the cost is high. TiO_2 prepared by chemical vapor deposition also has low photocatalytic activity.
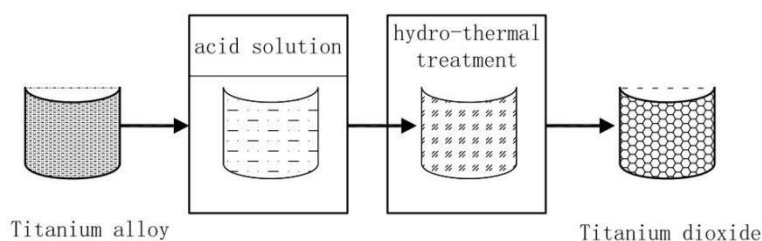
3.4. Hydrothermal synthesis

Figure 6. Preparation process of titanium dioxide by hydrothermal method[76]

The hydrothermal synthesis for preparing TiO_2 photocatalysts is described in Fig. 6. With this

technique, the substrate material and the TiO_2 precursor-containing aqueous solution are placed under high temperature and pressure to facilitate TiO_2 decomposition and precipitation on the substrate material surface. The crystal structure and surface morphology of TiO_2 can be controlled by introducing hydrothermal temperature [75], reaction time [76], precursor concentration [77] and surfactant [78], thereby improving the catalytic performance of photocatalysts. Fig. 7 illustrates the conventional process of preparing TiO_2 photocatalysts by hydrothermal synthesis. Exploiting this technique, Aydil [79] performed orientation growth on FTO glass to obtain single-crystal rutile TiO_2. Although the structure and crystal form of TiO_2 membranes can be regulated by hydrothermal synthesis, problems such as insufficient bonding force with the substrate and a wide pore size distribution of the membrane exist.

3.5. Anodizing

Fig. 7 displays a schematic of the equipment for preparing TiO_2 photocatalysts by anodization. Since titanium is a valve metal, when it is used as an anode and placed in an electrolyte, a TiO_2 membrane can be grown on its surface driven by an external electric field force. Since the anodizing preparation of TiO_2 nanotubes on titanium sheets by Zwilling [80] in 1999, the anodization technique has attracted extensive attention from scientists owing to the good adhesion to the substrate, simple operation, uniform texture and self-corrosion resistance of the prepared TiO_2 membranes. Ruan et al. [81] explored the photoelectric conversion efficiency of titanium nanotubes in 1 M KOH and borate electrolytes and found the values to be 6.8% and 7.9%, respectively. Schmuki [82] prepared a TiO_2 anodic oxide film in ferrous ammonium sulfate solution, where the microstructure and nanotube length of the TiO_2 photocatalyst were regulated by controlling the electrolyte composition and oxidation time. Therefore, TiO_2 photocatalysts with excellent performance were obtained. Zhang [83] prepared a TiO_2 membrane on a titanium metal surface in a NaOH electrolyte, thereby achieving regulation of the fiber network structure on the TiO_2 membrane surface, which exhibited a strong ability to degrade methylene blue. However, TiO_2 prepared by anodization techniques has problems such as a small absorption range of visible light and simple phase composition of catalysts, which result in insufficient efficiency of catalyst degradation.
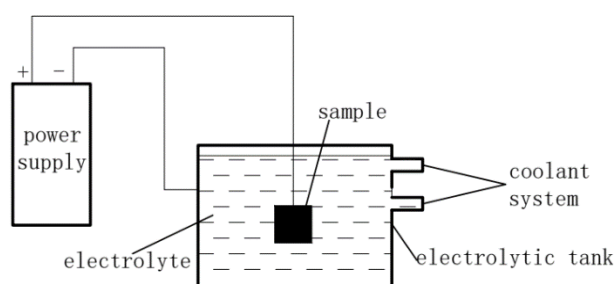

Figure 7. Preparation process of titanium dioxide by anodizing method[82]

4. CONCLUSION AND OUTLOOK

Conclusively, despite the rapid development of TiO$_2$ photocatalytic technology, it is still at an experimental and exploratory stage. Given the low utilization rate of sunlight by TiO$_2$, it can hardly treat high-concentration polluted wastewater. Traditionally, TiO$_2$ is mostly prepared as a powder, which is thus difficult to recycle. Although it can be loaded onto the carrier by immobilization, the effective catalytic area of catalysts is also reduced. Moreover, the treatment process is complicated, and the life cycle is short. Hence, broadening the photoabsorption range of TiO$_2$ and preparing highly active immobilized TiO$_2$ are the two major challenges. With ion doping techniques, seeking a reasonable doping measure can broaden the photoabsorption range of TiO$_2$, while reducing the photon–hole recombination rate is the key to improving the photocatalytic performance of TiO$_2$. With electrochemical techniques, the microstructure and phase composition of TiO$_2$ membranes are regulated during membrane preparation, which can greatly improve the catalytic performance of catalysts and simplify the wastewater treatment process.

References

1. A. Fujishima and K. Honda. *Nature,* 238 (1972) 37.
2. M. Choi, J. Lim, W. Choi, W. Kim and K.J. Yong. *ACS Appl. Mater. Interfaces,* 9 (2017) 16252.
3. K.Z. Qi, B. Cheng, J.G. Yu and W. Ho. *Chin. J. Catal.,* 38 (2017) 1936.
4. H.F. Yin, Y. Cao, T.L. Fan, B. Qiu and S. Chen. *J. Alloys Compd.,* 824 (2020) 153915.
5. X. Li, J. Sun, G. He, G. Jiang, Y. Tan and B. Xue. *J. Colloid Interface Sci.*, 411 (2013) 34.
6. C. Zhang, Q.L. Li and J.Q. Li. *Synth. Met.*, 160 (2010) 1699.
7. Q. Luo, X. Li, D. Wang and J. An. *J. Mater. Sci.*, 46 (2011) 1646.
8. F. Duan, Q. Zhang, D. Shi and M. Chen. *Appl. Surf. Sci.,* 268 (2013) 129.
9. A.F. Ghanem, A.A. Badawy, N. Ismail, Z.R. Tian, M.H.A. Rehim and A. Rabia. *Appl. Catal. A,* 472 (2014) 191.
10. M.R. Golobostanfard and H. Abdizadeh. *Microporous Mesoporous Mater.,* 183 (2014) 74.
11. X. Nie, G. Li, P. Wong and H. Zhao, *Catal. Today,* 230 (2014) 67.
12. L.M. Pastrana-Martínez, S. Morales-Torres, S.K. Papageorgiou, F.K. Katsaros, G.E. Romanos, J.L. Figueiredo, J.L. Faria, P. Falaras and A.M.T. Silva. *Appl. Catal. B-Environ.,* 142-143 (2013) 101.
13. P. Gao, Z. Liu, M. Tai, D.D. Sun and W. Ng. *Appl. Catal. B-Environ.,* 138-139 (2013) 17.
14. B. Long, J. Lin and X. Wang. *J. Mater. Chem. A,* 2 (2014) 2942.
15. H. Lee, B.J. Kim, Y.K. Park, J. Kim and S. Jung. *Catal. Today,* 355 (2020) 435.
16. C.S. Tsao, C.M. Chuang, C.Y. Chen, Y.C. Huang, H.C. Cha, F.H. Hsu, C.Y. Chen, Y.C. Tu and W.F. Su. *J. Phys. Chem. C,* 118 (2014) 26332.
17. R. Singh and S. Dutta. *Fuel,* 220 (2018) 15 607.
18. M. Gharagozlou and R. Bayati. *Ceram. Int.,* 40 (2018) 10247.
19. Y. Li, J. Wang, J.Y. Zhang, D. He, Q. An and G. Gao. *J. Hazard. Mater.,* 292 (2015) 79.
20. S. Leong, A. Razmjou, K. Wang, K. Hapgood, X. Zhang and H. Wang. *J. Membr. Sci.*, 472 (2014) 167.
21. J.B. Joo, Q. Zhang, M. Dahl, F. Zaera and Y. Yin. *J. Mater. Res.,* 28 (2013) 362.
22. W.Y. Choi, A. Terimn and M.R. Hoffmann. *J. phys. Chem. C,* 98 (1994) 13669.
23. N. Fajrina and M. Tahir. *Int. J. Hydrogen Energ.,* 44 (2019) 540.
24. A. Imran, S. mohd, Z.A. Alothman and A. Abdulrahman. *RSC Adv,* 8 (2018) 30125.
25. V. Kurnaravel, S. Mathew, J. Bartlett and S.C.Pillai. *Appl. Catal. B,* 244 (2019) 1021.

26. V.M. Menéndez-Flores and T. Ohno. *Catal. Today,* 230 (2014) 214.

27. O. Carp, C.L. Huisman and A. Reller. *Prog. Solid State Ch.,* 32 (2004) 33.

28. V. Etacheri, C.D. Valentin, J. Schneider, D. Bahnemann and S.C. Pillai. *J. Photochem. Photobiol. C,* 25 (2015) 1.

29. C. Acar, I. Dincer and C. Zamfirescu. *Int. J. Energ. Res.,* 38 (2014) 1903.

30. R. Nawaz, C.F. Kait, H.Y. Chia, M.H. Isa and L.W. Huei. *Environ. Technol.,* 19 (2020) 101007.

31. A. Houas, H. Lachheb, M. Ksibi, E. Elaloui, C. Guillard and J. Herrmann. *Appl. Catal. B,* 31 (2001) 145.

32. X.P. Wang and T.Lim. *Appl. Catal. B,* 100 (2010) 355.

33. D.Z. Li, Z.X. Chen, Y.L. Chen, W.J. Li, H.J. Huang, Y.H. He and X.Z. Fu. *Environ. Sci. Technol.,* 42 (2008) 2130.

34. Z.S. Guo, H. Wu, M. Li, T. Tang, J. Wen and X. Li. *Appl. Surf. Sci.,* 526 (2020) 146724.

35. H. Li, Y.B. Hao, H.Q. Lu, L.P. Liang, Y.Y. Wang, J.H. Qiu, X.C. Shi, Y. Wang and J.F. Yao. *Appl. Surf. Sci.,* 344 (2015) 112.

36. S.Y. Fang, Z.X. Sun and Y.H. Hu. *ACS Catal.,* 9 (2019) 5047.

37. H. Park, Y. Park, W. Kim and W. Choi. *J. Photochem. Photobiol. C,* 15 (2013) 1.

38. P. Mazierski, M. Nischk, M. Gołkowska, W. Lisowski, M. Gazda, W. Micha, T. Klimczuk and A. Zaleska-Medynska. *Appl. Catal. B,* 196 (2016) 77.

39. D. Li, H. Haneda , N. Labhsetwar, S. Hishita and N. Ohashi. *Chem. Phys. Lett.,* 401 (2005) 579.

40. J.Q. Yan, T. Wang, G.J. Wu, W. Dai, N. Guan, L. Li and J. Gong. *Adv. Mater.,* 27 (2015) 1580.

41. W. Wang, X.M. Xu, W. Zhou and Z.P. Shao. *Adv. Sci.,* 4 (2017) 1600371.

42. Y. Cao, Z.P. Xing, Y.C. Shen, Z. Li, X. Wu, X. Yan, J. Zou, S. Yang and Z. Wei. *Chem. Eng. J.,* 325 (2017) 199.

43. N. Nursam, X. Wang, J. Tan and R.A. Caruso. *ACS Appl. Mater. Interfaces,* 8 (1944) 17194.

44. N. Hirabuki, Y. Watanabe, T. Mano, N. Fujita, H. Tanaka, T. Ueguchi and H. Nakamura. *Am. J. Neuroradiol.,* 21 (2020) 1497.

45. C.D. Valentin, E. Finazzi, G. Pacchioni, A. Selloni and E. Giamello. *Chem. Mater.,* 20 (2008) 3706.

46. X.Q. Gong, A.A. Selloni, M. Batzill and U. Diebold. *Nat. Mater.,* 5 (2006) 665.

47. R. Asahi, T. Morikawa, T. Ohwaki, K. Aoki and Y. Taga. *Science,* 293 (2001) 269.

48. I. Nakamura, N. Negishi, S. Kutsuna, T. Ihara, S. Sugihara and K. Takeuchi1. *J. mol. Catal. A-Chem.,* 161 (2000) 205.

49. S. Sato. *Chem. Phys. Lett.,* 123 (1986) 126.

50. X. Zhang, K. Udagawa, Z. Liu, S. Nishimoto, C. Xu, Y. Liu, H. Sakai, M. Abe, T. Murakami and A. Fujishma. *J. Photoch. Photobio. A.,* 202 (2009) 39.

51. F. Meng, S.K. Cushing, J. Li, S. Hao and N. Wu. *ACS Catal.,* 5 (2015) 1949.

52. Y. Ide, N. Inami, H. Hattori, K. Saito, M. Sohmiya, N. Tsunoji, K. Komaguchi, T. Sano, Y. Bando and D. Golberg. *Angew. Chem. Int. Edit.,* 128 (2016) 3664.

53. C. Pan, T. Takata, M. Nakabayashi, T. Matsumoto and K. Domen. *Angew. Chem. Int. Edit.,* 127 (2015) 2998.

54. N. Tohge, K. Tadanaga, H. Sakatani and T. Minami. *J. Mater. Sci.,* 15 (1996) 1517.

55. X.J. Yu, L.L. Xiong, G.P. Ma, Y. Liang and K. Liu. *J. Rare Earth.,* 33 (2014) 26.

56. P. Karishma, C. Bahrim, S. Twagirayezu and T.J. Benson. *Adv. Catal.,* 66 (2020) 109.

57. J.M. Du, J.L. Zhang, Z.M. Liu，B.X. Han and Y. Huang. *Langmuir,* 22 (2006) 1307．

58. S.A. Ansari, M.M. Khan, M.O. Ansari and M.H. Cho. *New J. Chem.,* 39 (2015) 4708.

59. P.S. Awati, S.V. Awate, P.P. Shah and V. Ramaswamy. *Catal. Commun.,* 4 (2003) 393．

60. Q.H. Zhang, W.D. Han, Y.J. Hong and J.G. Yu. *Catal. Today,* 148 (2009) 335.

61. C. Belver, M.J. Lopez-Muoz, J.M. Coronado and J. Soria. *Appl. Catal., B-environ.,* 46 (2003) 497．

62. C.K. Jung, S.H. Cho, S.B. Lee , T.K. Kim, M.N. Lee and J.H. Boo. *Surf. Rev. Lett.,* 10 (2008) 635.

63. S. Kurajica, J. Macan, V. Mandic, M. Galjer, K. Mužina and J.R. Plaisier. *Mater. Res. Bull.,* 105 (2018) 142.

64. B. Cangul, L.C. Zhang, M. Aindow and C. Erkey. *J. Supercrit. Fluids,* 50 (2009) 82.
65. R.Y. Chen, V. Trieu, B. Schley, H. Natter, J. Kintrup, A. Bulan, R. Weber and R. Hempelmann. *Z. Phys. Chem.,* 227 (2013) 651.
66. L. Guo, L.B. Huang, W.J. Jiang and Z.D. Wang. *J. Mater. Chem. A,* 5 (2000) 9014.
67. M.C. Vebber, A.C.R. Faria, N. DalAcqua, L.L. Beal, G. Fetter, G. Machado, M. Giovanela and J.S. Crespo. *Int. J. Hydrogen Energy,* 41 (2016) 17995.
68. L.L. Li, B. Cheng, Y.X. Wang and J. Yu. *J. Colloid Interface Sci.,* 449 (2015) 115.
69. S. Obregon, M.J. Munoz-Batista, M. Fernandez-Garcia, A. Kubacka and G. Colón. *Appl. Catal. B,* 179 (2015) 468.
70. P. Srivastava and L. Bahadur. *Int. J. Hydrogen Energy,* 37 (2012) 4863.
71. M. Kitano and M. Hara. *J. Mater. Chem.,* 20 (2010) 627.
72. J. Liu, L. Yang, N. Liu, Y. Han, Z. Xing, H. Huang, Y. Lifshitz, S.T. Lee, J. Zhong and Z. Kang. *Science,* 347 (2015) 970.
73. S. Ghosh, N.A. Kouame, L. Ramos, S. Remita, A. Dazzi, A. Deniset-Besseau, P. Beaunier, F. Goubard, P.H. Aubert and H. Remita. *Nat. Mater.,* 14 (2015) 505.
74. J.B. Fei and J.B. Li. *Adv. Mater.,* 27 (2014) 314.
75. R. Fagan, D.E. McCormack, S. Hinder, S. Hinder and S.C. Pillai. *Mater. Design,* 96 (2016) 44.
76. A.A. Ismail and D.W. Bahnemann. *Sol. Energy. Mater. Sol. C.,* 128 (2014) 85.
77. M.T. Chao and A.R. Mohamed. *J. Alloys Compd.,* 509 (2011) 1648.
78. R. Jaiswal, J. Bharambe, N. Patel, A. Dashora, D.C. Kothari and A. Miotello. *Appl. Catal. B,* 168 (2015) 333.
79. S. Kuriakose, B. Satpati and S. Mohapatra. *Phys. Chem. Chem. Phys.,* 17 (2015) 2517225181.
80. R. Abe. *J. Photoch. Photobio. C,* 11 (2010) 179.
81. J. Yuan, M.X. Chen, J.W. Shi and W.F. Shangguan. *Int. J. Hydrogen Energy,* 31 (2006) 1326.
82. M.N. Chong, B. Jin, C.W.K. Chow and C. *Water Res.,* 44 (2010) 2997.
83. Y. Zhang, Z.Y. Zhao, J.R. Chen, L. Cheng, J. Chang, W.C. Sheng, C.Y. Hu and S.S. Cao. *Appl. Catal. B,* 165 (2015) 715.